Journal of Clinical & Experimental Ophthalmology

Di Staso et al., J Clin Exp Ophthalmol 2016, 7:1
http://dx.doi.org/10.4172/2155-9570.1000524

Research Article Open Access

In Vivo Three-Dimensional Analysis of Conjunctival Epithelial Microcysts in Glaucoma

Silvio Di Staso[1], **Marco Ciancaglini**[1], **Luca Agnifili**[2*], **Vincenzo Fasanella**[2], **Mario Nubile**[2], **Rodolfo Mastropasqua**[3] **Emilio Galassi**[1] **and Leonardo Mastropasqua**[2]

[1]*Ophthalmology Unit, Department of Life, Health and Environmental Sciences, University of L'Aquila, 67100, Italy*

[2]*Ophthalmic Clinic, Department of Medicine and Aging Science, University G. d'Annunzio of Chieti-Pescara, Chieti, 66100, Italy*

[3]*Ophthalmology Unit, Department of Neurological, Neuropsychological, Morphological and Movement Sciences, University of Verona, 37100, Verona, Italy*

[*]**Corresponding author:** Luca Agnifili, Ophthalmology Clinic, 114, 66100 Chieti, Italy, Tel: +39-0871-358410; Fax: +39-0871-358794; E-mail: l.agnifili@unich.it

Received date: December 26, 2015; **Accepted date:** February 15, 2016; **Published date:** February 18, 2016

Abstract

Objective: To analyze the three-dimensional (3D) features of conjunctival epithelial microcysts (CEM) in eyes affected with primary open angle glaucoma (POAG).

Methods: This was a case series study. Nine patients that underwent successful trabeculectomy and four eyes with medically controlled POAG were enrolled. Patients were examined with confocal laser-scanning microscope (Heidelberg Retina Tomograph/Rostock Cornea Module). Sequential images 300 × 300 µm (384 × 384 pixels) derived from automatic scans were acquired throughout the upper bulbar conjunctiva, 2 mm from the limbus. Image acquisition was performed in z-scan automatic volume mode and a series of 40 images to a maximum depth of 40 µm were captured. The 3-D volume tissue reconstruction with a maximal size of 300 × 300 × 40 µm and voxel size of 0.78 × 0.78 × 0.95 µm was performed with the AMIRA volume-rendering software package, to provide a 3-D characterization of conjunctival epithelial microcysts (CEM).

Results: In the enface view, CEM appeared as empty, optically clear, round or oval shaped sub-epithelial structures. In eyes that underwent trabeculectomy CEM showed greater density and larger area compared to medically controlled glaucomatous eyes. The 3-D spatial reconstruction showed microcysts as oval-shaped, optically clear, differently sized structures, often surrounded by a well-defined and mildly thick wall. All microcysts were embedded in the extra cellular spaces and located 10 µm below the epithelial surface.

Conclusions: Conjunctival epithelial microcysts were proposed as hallmark of trans-scleral aqueous humor outflow in eyes with glaucoma. They can be effectively imaged with a 3-D reconstruction system, which permits to better clarify their microscopic anatomy and patho-physiological significance.

Keywords: *In vivo* confocal microscopy; Primary open angle glaucoma; Trans-scleral aqueous humor outflow; Trabeculectomy; Conjunctival microcysts; Three-dimensional analysis

Introduction

The *in vivo* confocal microscopy (IVCM), impression cytology (IC), and immuno-histology provided crucial information of the conjunctiva in patients with glaucoma. Several studies documented that IVCM proved valuable in the functional assessment of filtering bleb after trabeculectomy, by evaluating conjunctival epithelial microcysts (CEM), the sub-epithelial connective tissue, and blood vessels [1-7]. Functioning blebs had more microcysts in the conjunctival epithelium compared to non-functioning blebs, in which these structures were rare, small and scattered. Microcysts were intended as vesicles of aqueous humor (AH) percolating the bleb-wall. Based on these findings the presence of a high density and area CEM were proposed as an indicator of functioning blebs. Amar et al., in an IVCM and immuno-histological study [8], further demonstrated that microcysts observed at the surface of functioning blebs seemed to correspond to goblet cells, mostly containing aqueous humor instead of highly hydrophilic gel-forming mucins. In this study it was hypothesized that AH percolation occurs at the level of goblet cells, which act as carriers.

The presence of CEM is not limited to trabeculectomized eyes since they were described also in untreated ocular hypertension (OH), in medically treated open glaucoma, and also in bleb-less procedures [9-14]. The *in vivo* detection of these structures in such a wide range of glaucomatous conditions, allowed considering them as a hallmark of AH passage through the sclera and the conjunctiva.

In this study we analyzed the three-dimensional (3-D) features of CEM in medically treated and trabeculectomized patients with open angle glaucoma, to improve the knowledge of the morphological characteristics and physiology of these structures.

Material and Methods

This was an observational, non-randomized, institutional, case series study that adhered to the tenets of the Declaration of Helsinki. Informed consent was obtained from all subjects after explanation of the nature and possible consequences of the methods used in the study; our Institutional Review Board approved the project. A 3-D *in vivo* microscopic technique using the Heidelberg Retina Tomograph II,

(Heidelberg Engineering, Germany) in combination with an anterior segment adapter (Rostock Cornea Module) was utilized to shift the focal plane into conjunctiva of glaucomatous eyes. Technical characteristics of this instrument and the details of conjunctival examination were previously described [5].

We examined 9 eyes of Caucasian patients affected with primary open angle glaucoma (POAG), 5 eyes (3 right and 2 left eyes) of 5 patients (3 males and 2 females, age ranging from 48 to 70 years; mean of 61.3 ± 4.2 years) who underwent successful fornix based flap trabeculectomy [5] (intraoperative mitomycin C (MMC) 0.2 mg/mL for was applied for 2 min on the sclera at the site where the flap was outlined), and 4 eyes (2 right and 2 left eyes) of 4 subjects (2 males and 2 females, age ranging from 50 to 64; mean age 57.5 ± 3.6 years) with medically controlled glaucoma.

For the surgically treated patients, inclusion criteria were the following: preoperative uncontrolled IOP (≥ 22 mmHg, mean of three measurements at 9 AM, 12 noon and 4 PM) under maximal tolerated medical therapy, topical hypotensive therapy started at least 12 months before surgery, progression of glaucomatous damage confirmed on three consecutive SITA standard 30-2 visual fields (Humphrey field analyzer II 750; Carl Zeiss Meditec, Inc., Dublin, CA, USA). The results of surgery were classified as success if a reduction of one-third of preoperative IOP without medical treatment [5] and IOP lower than 18 mmHg were achieved. Post-surgical therapy required unpreserved topical steroids for 4 weeks (unpreserved dexamethasone 0.15% eye drops four times a day for 2 weeks and three-time daily for the following 2 weeks) and topical antibiotic for 2 weeks (ofloxacin 0.3% fourfold daily). IVCM examination was performed 5 weeks after trabeculectomy that is one week after cessation of any topical therapy. For medically controlled patients, inclusion criteria were the followings: IOP lower than 18 mmHg (mean of three time-points measurements at 9 AM, 12 noon and 4 PM), therapy with unpreserved prostaglandin analogues for at least 6 months, presence of classic ophthalmoscopic signs of glaucomatous optic neuropathy and glaucomatous visual-field defects.

For both groups exclusion criteria were: best corrected visual acuity ≤ 20/40, refractive error ≥ 4 dioptres (spherical equivalent), central corneal thickness <530 and >560 μm, pseudo-exfoliation, end-stage glaucoma (mean deviation >15 dB), visual-field defects attributable to non-glaucomatous conditions, history of angle closure or an occludable angle on gonioscopy, argon laser trabeculoplasty or laser iridotomy, previous surgical procedure for glaucoma, aphakia, history or signs of inflammatory eye disease, uveitic glaucoma, ocular trauma, the presence of dry eye or other ocular disease during the previous 12 months.

A single operator (SDS) carefully examined each glaucomatous eye using Confocal Laser-Scanning Microscope. Confocal microscopy was carried out under topical anesthesia with 0.4% oxybuprocaine. Sequential images 300 × 300 μm in size (384 × 384 pixels), derived from automatic scans were acquired of the upper bulbar conjunctiva of each examined eye, 2 mm from the limbus, in downward gaze. An internal scanning device moving the focal plane perpendicularly to the x-y-plane, in a similar way to HRT II optic disc topography was used to obtain the 3-D images. During the image capture process, the z-movement is stopped and the image plane is exactly perpendicular to the z-axis. Image acquisition was performed in z-scan automatic volume mode and a series of maximal 40 images to a maximum depth of 40 μm were captured. The image acquisition time for a single frame was 0.025 seconds, with a total acquisition time for a 3-D image stack of 1.2 seconds. Longer acquisition times create important biases in final 3-D image generation due to patient and examiner movements.

To overcome the misalignment of each single frame, a semiautomatic image alignment using a least-square algorithm based on grey values was performed according to indications of Stachs et al. [15]. After this the procedure a 3-D reconstruction of a tissue volume with a maximal size of 300 × 300 × 40 μm and a voxel size of 0.78 × 0.78 × 0.95 μm was obtained by using the AMIRA volume-rendering software package (AMIRA 5.4 (TGS Inc., USA). Volume orientation for viewing planes and 3-D perspectives segmentation, enface view, determination of distances, cross-section and oblique section were generated to assess the conjunctival epithelium microcysts in sufficiently high quality. The great speed and the uniform illumination of the images made 3-D reconstruction possible since the single frame quality remained good even in deep scans.

Results

Depending on the patient compliance and the amplitude of saccadic eye movements, about the 50% of all 3-D data sets were rejected because of artefacts. The morphology of the conjunctival epithelium, microcysts and sub-epithelial tissue were analyzed by IVCM in a single section in both groups (Figures 1 and 2).

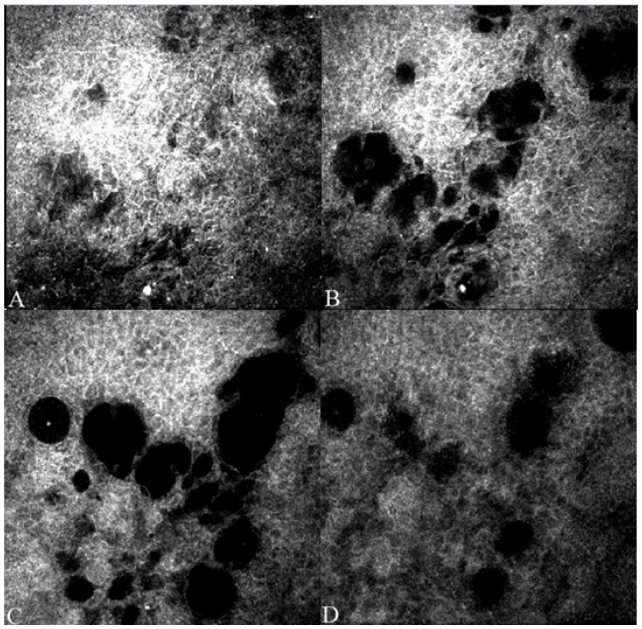

Figure 1: Enface views of conjunctiva in surgically treated eyes at the surface (A), 10 μm (B), 15 μm (C), and 20 μm (D) below show a large number of microcysts and their changes in size at different focal plans.

In the enface view conjunctival microcysts appeared as optically clear, dark, round or oval shaped structures located below the epithelium. Patients that underwent trabeculectomy showed microcysts with a greater density and larger area, sometimes confluent or clustered, compared to medically controlled patients. In medically controlled treated patients the mean microcyst density (MMD, cysts/mm^2) and area (MMA, μm^2) were 11.61 ± 3.21 and 2715 ± 31, respectively. In patients who underwent trabeculectomy MMD and

MMA were markedly greater, with values of 95.1 ± 24.3 and 25387 ± 12954.9, respectively.

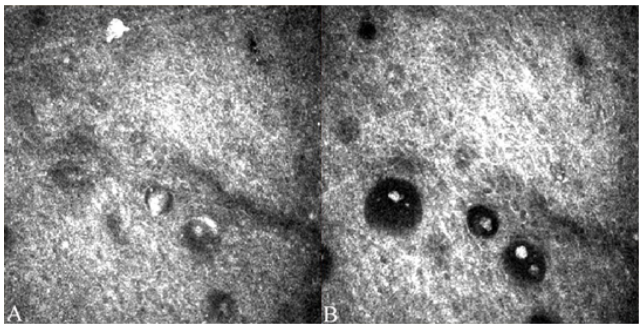

Figure 2: Enface views of conjunctiva in medically treated eyes at the surface (A), 10 µm below (B), show a small amount of microcysts that present a partially hyperreflective inner cavity due to the accumulation of amorphous material. Figure 2: Enface views of conjunctiva in medically treated eyes at the surface (A), 10 µm below (B), show a small amount of microcysts that present a partially hyperreflective inner cavity due to the accumulation of amorphous material.

Data from the confocal microscopy corresponded to a series of maximal 40 two-dimensional grey-scale images representing optical sections through the conjunctiva. The 3-D analysis documented an anatomical relationship of microcysts with epithelium and sub-epithelium: the oblique section and z scans revealed that CEM were very close, but clearly separated from the epithelium (Figure 3). The 3-D reconstruction confirmed that microcysts were oval-shaped, optically clear and differently sized, often surrounded by a well-defined and mildly thick wall (capsule). All microcysts were embedded in the extra cellular matrix and located about 10 µm below the epithelial surface (Figures 4 and 5). CEM size was different in the two groups, being smaller in medically treated eyes (range 10-15 µm) and larger in surgically treated eyes (range 20-25 µm). No extracellular or canal structures were recognized below the microcysts.

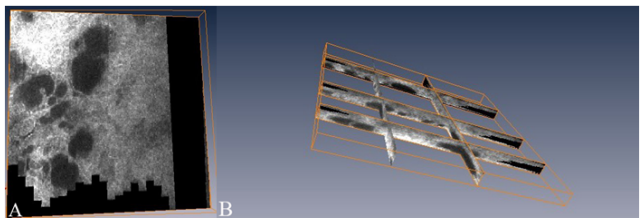

Figure 3: Oblique scan (A) and multiple z scans (B) reveal that conjunctival epithelium and microcysts, which are independent and clearly separate structures.

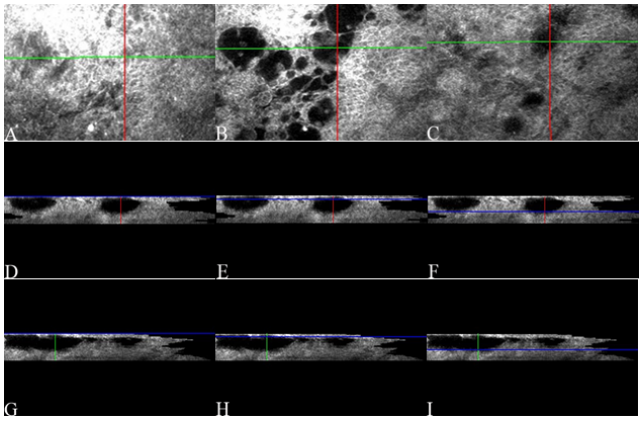

Figure 4: 3-D analysis at superficial (A), intermediate (B), and deep layer (C) of surgically treated eyes, showing oval shaped microcysts in Y (D, E, F red line) and X scans (G, H, I, green line) with a 24 µm size. The blue line identifies the scan plane with respect to the surface (top image).

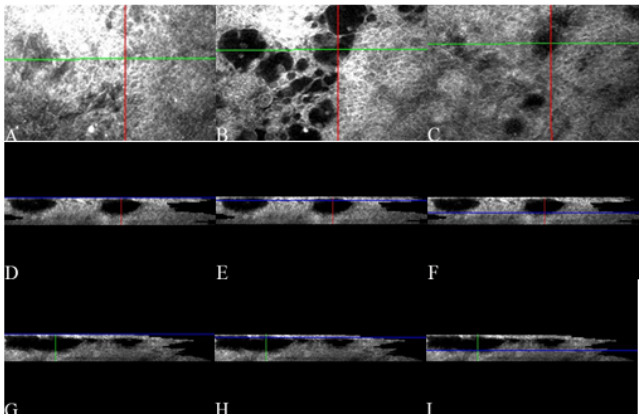

Figure 5: 3-D analysis at superficial (A) and deep layer (B) (red line) of medically treated eyes, showing smaller (12 µm) microcysts with respect to surgically treated eyes in Y (C, D green line) and X scans (E, F, blue line). The red line identifies the scan plane with respect to the surface (top image).

Discussion

Over the past years, knowledge about the ocular surface in glaucoma has greatly increased through the use of *in vivo* confocal microscopy [1-14]. This technique was used to describe the impact of the IOP lowering medications on the development of the glaucoma-related ocular surface disease, to evaluate the anatomy and functionality of conjunctival blebs after filtration surgery, and to study the patho-physiology of the AH along the uveo-scleral outflow pathway. In these two fields of research, IVCM documented the presence of CEM, which progressively gained the significance of a glaucoma hallmark. The presence of CEM in eyes that underwent surgery is consistent with clinical biomicroscopy and with histology, in which several epithelial cysts are commonly found within the bleb-wall

epithelium of functioning trabeculectomy [16]. Compared to slit-lamp evaluation, which provides limited information on the drainage ability of a bleb, IVCM permitted a significant advancement in the filtration assessment, since indicated microcysts as objective features associated with success or failure.

Such microcysts, which were intended as micro-blebs filled with AH, were also described within the conjunctival epithelium of untreated OH or medically controlled glaucomatous patients, even if with slightly different features. In OH and in POAG they were described smaller (10-90 μm) than those observed after filtering surgery (10-300 μm), quite regularly distributed within the epithelium, and without a tendency of clustering. The presence of CEM in POAG and OH, despite a huge inter-individual variability, was interpreted as an adaptive mechanism in presence of a reduced trabecular outflow, aimed at increasing the AH movement through the sclera and, finally, conjunctiva.

However, CEM were occasionally described in healthy subjects [10,17-19] and in some non-glaucomatous ocular conditions such as pterygium, Sjogren' s syndrome, contact lens wearing [17-19]. In these cases, CEM were intended as expression of degenerative processes occurring within the epithelium, when disorders in cellular maturation created debris field cystic spaces.

The presence of these structures in healthy eyes could correspond to degenerated goblet cells, or normal intermediate products that result from cellular development and maturation [19]. On the other hand, in normal eyes, CEM could be a sign of physiological trans-scleral AH percolation, which normally occurs at the end of the uveo-scleral pathway [10]. Therefore, CEM may have more than one connotation: it may be expression of the physiologic trans-scleral AH outflow or an aspect of the goblet cell maturation in healthy conditions, a hallmark of the trans-scleral outflow in OH or glaucoma, and a sign of epithelial alteration in patients with non-glaucomatous ocular surface diseases.

The 3-D analysis of the ocular surface epithelia was initiated by Zhivov et al. [20], who used a novel polymethyl methacrylate (PMMA) contact cap to minimize artifacts due to applanation pressure during the confocal examination. The authors reported that this technique permitted an accurate analysis of the corneal surface and corneal epithelium capable to give information about the spatial arrangement at the cellular level in normal and pathological corneas.

In our study, the 3-D characterization of the conjunctiva provided additional information on the comprehension of CEM anatomy and functionality. In the present study, CEM appeared similar to those previously reported in 2-D confocal microscopy studies, [1-14] where their oval or round shaped features were indicative of the possible 3-D feature. The 3-D reconstruction described microcysts as spherical, ovoid, and differently sized micro-blebs, embedded in the extra cellular matrix, mostly located below the epithelial surface rather than within the epithelial layers.

This may indicate that the origin of CEM is stromal and not epithelial, in opposition to results of Amar et al., who recognized microcysts as modified goblet cells [8]. Independently from the origin, they can be intended as changing structures, moving from the deep stroma to the superficial layers of the epithelium, with the intent to transport the AH towards the ocular surface.

The different 2-D and 3-D morphological aspect of CEM in medically treated and trabeculectomized glaucomatous eyes, could derive from the characteristics of the AH passage through tissues with a different anatomy. The turbulence of the AH through the bleb cavity and the bleb-wall, which is constituted by loosely arranged conjunctival tissue in functioning cases, may account for the greater dimension and for the clustering tendency of CEM. On the other hand, the regular anatomy of the human sclera with thickly arranged collagen fibers, could account for smaller and dispersed microcysts in the conjunctiva of medically treated patients.

The present study presents some limitations, mostly related to the 3-D analysis process. First: the image capture and data examination require a great attention, to obtain a good alignment and high quality images. The single images are often misaligned between them, due to eye movements during the acquisition process. However, automated or manual intervention can be performed using the Align Slice Module of AMIRA software; in the worst case, when the alignment process fails and part of the individual slices leave the target area, a dark field appears (Figure 3; bottom of the image A). When the misalignment is limited to a small part of the scanned volume (300 × 300 × 40 μm) the quality of 3D reconstruction is sufficient to allow a good anatomic examination of the tissue. At the end of the process, the 50% of data cannot be used for 3-D analysis.

Second: the examination could cause artifacts due to mechanical pressure exerted on the conjunctival surface by the cornea module during the acquisition process. Even though the front lens of the objective is coupled with the cornea via a PMMA cup with interposition of transparent gel, we cannot exclude the induction of a mild microcyst deformation and shape modifications.

Finally, we did not consider failed blebs, since CEM in these cases are rare and small; further studies comparing the 3-D features of microcysts in successful and unsuccessful blebs may potentially add new information on the patho-physiology of filtration failure.

Similarly, further studies focused on the 3-D reconstruction of CEM also in non-glaucomatous conditions are warranted to reveal microscopic changes between different diseases, useful to better clarify the role of these structures in each situation in which they appear.

The 3-D analysis of the conjunctiva should be further extended to other cellular and non-cellular tissue components, especially in the bleb-wall, since it could clarify the mechanisms of failure from a different point of view, integrating the current information of the filtering bleb physiology.

References

1. Labbé A, Dupas B, Hamard P, Baudouin C (2005) In vivo confocal microscopy study of blebs after filtering surgery. Ophthalmology 112: 1979.
2. Messmer EM, Zapp DM, Mackert MJ, Thiel M, Kampik A (2006) In vivo confocal microscopy of filtering blebs after trabeculectomy. Arch Ophthalmol 124: 1095-1103.
3. Guthoff R, Klink T, Schlunck G, Grehn F (2006) In vivo confocal microscopy of failing and functioning filtering blebs: Results and clinical correlations. J Glaucoma 15: 552-558.
4. Ciancaglini M, Carpineto P, Agnifili L, Nubile M, Lanzini M, et al. (2008) Filtering bleb functionality: a clinical, anterior segment optical coherence tomography and in vivo confocal microscopy study. J Glaucoma 17: 308-317.
5. Ciancaglini M, Carpineto P, Agnifili L, Nubile M, Fasanella V, et al. (2009) Conjunctival characteristics in primary open-angle glaucoma and modifications induced by trabeculectomy with mitomycin C: an in vivo confocal microscopy study. Br J Ophthalmol 93: 1204-1209.

6. Mastropasqua L, Agnifili L, Mastropasqua R, Fasanella V (2013) Conjunctival modifications induced by medical and surgical therapies in patients with glaucoma. Curr Opin Pharmacol 13: 56-64.
7. Carpineto P, Agnifili L, Nubile M, Fasanella V, Doronzo E, et al. (2011) Conjunctival and corneal findings in bleb-associated endophthalmitis: an in vivo confocal microscopy study. Acta Ophthalmol 89: 388-395.
8. Amar N, Labbé A, Hamard P, Dupas B, Baudouin C (2008) Filtering blebs and aqueous pathway an immunocytological and in vivo confocal microscopy study. Ophthalmology 115: 1154-1161.
9. Ciancaglini M, Carpineto P, Agnifili L, Nubile M, Fasanella V, et al. (2008) Conjunctival modifications in ocular hypertension and primary open angle glaucoma: an in vivo confocal microscopy study. Invest Ophthalmol Vis Sci 49: 3042-3048.
10. Agnifili L, Carpineto P, Fasanella V, Mastropasqua R, Zappacosta A, et al. (2012) Conjunctival findings in hyperbaric and low-tension glaucoma: an in vivo confocal microscopy study. Acta Ophthalmol 90: e132-137.
11. Mastropasqua R, Fasanella V, Pedrotti E, Lanzini M, Di Staso S, et al. (2014) Trans-conjunctival aqueous humor outflow in glaucomatous patients treated with prostaglandin analogues: an in vivo confocal microscopy study. Graefes Arch Clin Exp Ophthalmol 252: 1469-1476.
12. Mastropasqua L, Agnifili L, Salvetat ML, Ciancaglini M, Fasanella V, et al. (2012) In vivo analysis of conjunctiva in canaloplasty for glaucoma. Br J Ophthalmol 96: 634-639.
13. Mastropasqua L, Agnifili L, Ciancaglini M, Nubile M, Carpineto P, et al. (2010) In vivo analysis of conjunctiva in gold micro shunt implantation for glaucoma. Br J Ophthalmol 94: 1592-1596.
14. Mastropasqua L, Agnifili L, Mastropasqua R, Fasanella V, Nubile M, et al. (2014) In vivo laser scanning confocal microscopy of the ocular surface in glaucoma. Microsc Microanal 20: 879-894.
15. Stachs O, Zhivov A, Kraak R, Stave J, Guthoff R (2007) In vivo three-dimensional confocal laser scanning microscopy of the epithelial nerve structure in the human cornea. Graefe's Arch Clin Exp Ophthalmol 245: 569-575.
16. Addicks EM, Quigley HA, Green WR, Robin AL (1983) Histologic characteristics of filtering blebs in glaucomatous eyes. Arch Ophthalmol 101: 795-798.
17. Wakamatsu TH, Sato EA, Matsumoto Y, Ibrahim OM, Dogru M, et al. (2010) Conjunctival in vivo confocal scanning laser microscopy in patients with Sjögren syndrome. Invest Ophthalmol Vis Sci 51: 144-150.
18. Efron N, Al-Dossari M, Pritchard N (2010) Confocal microscopy of the bulbar conjunctiva in contact lens wear. Cornea 29: 43-52.
19. Zhu W, Hong J, Zheng T, Le Q, Xu J, et al. (2010) Age-related changes of human conjunctiva on in vivo confocal microscopy. Br J Ophthalmol 94: 1448-1453.
20. Zhivov A, Stachs O, Stave J, Guthoff RF (2009) In vivo three-dimensional confocal laser scanning microscopy of corneal surface and epithelium. Br J Ophthalmol 93: 667-672.